Available online at www.sciencedirect.com
SCIENCE DIRECT
Biochemical Pharmacology 69 (2005) 981–991
Biochemical Pharmacology
www.elsevier.com/locate/biochempharm

Biodistribution and metabolism of immunostimulatory oligodeoxynucleotide CPG 7909 in mouse and rat tissues following subcutaneous administration

Bernhard O. Noll [a,*], Michael J. McCluskie [b], Tanja Sniatala [a], Angela Lohner [a], Stephanie Yuill [b], Arthur M. Krieg [c], Christian Schetter [a], Heather L. Davis [b], Eugen Uhlmann [a]

[a] *Coley Pharmaceutical GmbH, Elisabeth-Selbert-Strasse 9, D-40764 Langenfeld, Germany*
[b] *Coley Pharmaceutical Group, 340 Terry Fox Drive, Suite 200, Kanata, Ottawa, Ont., Canada K2K 3A2*
[c] *Coley Pharmaceutical Group Inc., 93 Worcester Street, Suite 101, Wellesley, MA 02481, USA*

Received 30 September 2004; accepted 28 December 2004

Abstract

To evaluate pharmacokinetics (PK) and biodistribution, CPG 7909, a 24-mer immunostimulatory fully phosphorothioated oligodeoxynucleotide (PS-ODN), was administered by subcutaneous injection at 2, 5 and 12.5 mg/kg to mice and at 9 mg/kg to rats. Parent compound and metabolites were isolated from plasma and tissues and quantified by capillary gel electrophoresis with UV detection (CGE-UV) and molecular masses were determined by matrix-assisted-laser-desorption-ionization time of flight detection (MALDI-TOF). An established method for PS-ODN isolation from plasma and tissue was modified to prevent oxidation of the phosphorothioate bonds during the extraction process, significantly increasing sensitivity in the subsequent MALDI-TOF analysis. Concentrations of CPG 7909 and metabolites were highest at the injection site (>600 mg/kg at 4 h). Maximal concentrations in local (draining) lymph nodes (LLN), kidney and liver were 10–15% of that at the injection site. The highest total amount of PS-ODN (percentage of administered dose) was found in the liver (32% at 4 h), followed closely by the injection site (23% at 4 h). Only very low levels of CPG 7909 and metabolites were found in plasma and only during the first hours. Metabolites identified by MALDI-TOF were similar for both species and all analyzed tissues, although the relative amounts of the different metabolites varied with tissue and over time. Degradation of CPG 7909 in vivo occurred predominantly by 3′exonucleases with additional cleavage by endonucleases.

Keywords: Oligonucleotide; Metabolites; Pharmacokinetics; Capillary gel electrophoresis; MALDI-TOF; Solid phase extraction

1. Introduction

CPG 7909, also known as CpG 2006, is a 24 mer PS-ODN containing three human-optimized immunostimulatory 6 mer CpG motifs and made with a fully phosphorothioate backbone to render it more nuclease resistant [1,2]. CPG 7909 is being developed as a novel first generation drug candidate for immune therapy in cancer indications [3] and is currently in Phase II human clinical trials in non-small cell lung cancer, melanoma and cutaneous T cell lymphoma. CPG 7909 is also being tested as an adjuvant for infectious disease and cancer vaccines [4–6]. Doses in the oncology clinical trials range from 0.08 to 0.64 mg/kg, while adjuvant doses tested range from 0.125 to 1 mg (approximately 0.002–0.01 mg/kg).

PK and tissue distribution of PS-ODN have been described after intravenous, intradermal, intraperitoneal, subcutaneous and intrapulmonary administration [7–21] in odents [10,22–25], primates [12,26–29] and humans

Abbreviations: ODN, oligodeoxynucleotide; PS-ODN, fully phosphorothioated oligodeoxynucleotide; PK, pharmacokinetics; IV, intravenous; SC, subcutaneous; CGE-UV/LIF, capillary gel electrophoresis with UV or laser induced fluorescence detection; MALDI-TOF, matrix-assisted-laser-desorption-ionization time of flight detection; SPE, solid phase extraction; HPLC/ESI-MS, high-performance-liquid-chromatography/electro-spray-ionization-mass-spectrometry; LLN, local (draining) lymph nodes; DTT, 1,4-dithio-DL-threitol

* Corresponding author. Tel.: +49 2173 3997 2231; fax: +49 2173 3997 2399.
E-mail address: bnoll@coleypharma.com (B.O. Noll).

0006-2952/$ – see front matter © 2005 Elsevier Inc. All rights reserved.
doi:10.1016/j.bcp.2004.12.013

[30–34]. The PK of various PS-ODN have been reported to be dose dependent, sequence independent and equivalent on a dose per body weight basis across non-human and human species, and it is generally accepted that plasma PK in humans can be extrapolated from other species [23,33]. However, a direct species comparison [28] reported that after IV administration, plasma clearance and distribution half-life were more rapid, and drug concentrations in the major organs of deposition (liver, kidney and spleen) were much lower in mice than monkeys. In plasma, approximately 91–99% of PS-ODN is protein bound with the major protein species being albumin and α2-macroglobulin [35,10].

Although PS-ODN are more resistant to degradation by nucleases relative to oligonucleotides made with an unmodified phosphodiester backbone, degradation does still occur. In general, it is reported that 3′exonucleases are the major degradation pathway [36,37,23,38]. Degradation at early times appears to be rapid with a high percentage of metabolites being detected in the plasma as early as 10 min, however, degradation seems to progress more slowly at later times [19]. Explanations for this include the inhibition of nucleases [14] and/or the distribution of Rp and Sp phosphorothioate diastereoisomeres, which have significantly different nuclease resistance [39,40,41]. Degraded PS-ODN are eliminated primarily by urinary excretion [29,42]. Reports from various clinical studies appear to obtain different pharmacokinetic profiles, however this is likely due in large part to the different analytical techniques used; some methods measure only parent compound, whereas others detect both parent and chain-shortened metabolites. Furthermore, there have been very few studies that have attempted to evaluate metabolite profiles of PS-ODN including identification of metabolites in solid organs. The reported techniques for these studies include CGE-UV/LIF, MALDI-TOF [43], HPLC/ESI-MS [44,45], CGE and ion-pair-reversed-phase-HPLC followed by ESI-MS [46,47] and CGE-UV/ESI [19].

While detection of only full-length PS-ODN may be sufficient for antisense drugs, where virtually all metabolites are expected to be inactive, this is not the case for CPG 7909. Since CPG 7909 contains several hexanucleotide CpG motifs, some of its metabolites also show immunomodulatory properties (Vollmer, unpublished results). Therefore, it is of great interest to identify and quantify the main metabolites of CPG 7909 in the major organs of ODN distribution. Herein we have examined rat and mouse liver, kidney, local lymph nodes and spleen tissues after subcutaneous (SC) administration of CPG 7909 and identified the major metabolites present at various times. For this we have used several techniques including CGE-UV and MALDI-TOF. We also describe a modified method for SPE for PS-ODN that avoids oxidation at the phosphorothioate bonds, a problem that heretofore caused problems for interpreting mass-spectroscopy data of isolated metabolites, as had been observed by us and others [19,43].

2. Methods

2.1. Test article

CPG 7909 is a 24 mer full phosphorothioate oligodeoxynucleotide with the sequence 5′-TCG TCG TTT TGT CGT TTT GTC GTT-3′. The internal control (IS) is a 31 mer full phosphorothioate oligodeoxynucleotide with the sequence 5′-TTT TTT TTT TTT TTT TTT TTT TTT TTT TTT T-3′. The CPG 7909 was manufactured by Avecia Biotechnology and the IS was manufactured at Coley Pharmaceutical GmbH.

2.2. Test system

Male and female Sprague–Dawley rats (∼200 g) and female Balb/c mice (∼20 g) were obtained from Charles River. Rats were housed in same sex pairs and mice in groups of up to five mice per cage. During the test period, animals were fed a standard laboratory diet and kept under controlled conditions. All studies were conducted in the Animal Care Facility of Coley Pharmaceutical Group. All animal experiments were subject to approval by the Coley Canada Animal Care Committee, under the guidelines and requirements of the Canadian Council on Animal Care (CCAC).

2.3. Test article administration

All animals were weighed immediately prior to dosing. All animals received the indicated dose of CPG 7909 in a total volume of either 2.5 ml/kg (rats) or 0.1 ml (mice). All administrations were given under light isofluorane anaesthetic. Administration was by single SC bolus injection.

2.4. Sample collection

Plasma: blood samples (∼0.5 ml) were collected after 10 and 30 min, and 1, 2, 4 and 8 h via the tail artery after anaesthetization with isofluorane, and centrifuged at 13,000 rpm for 10 min to enable plasma collection. Plasma samples were stored at $\leq -15\ ^{\circ}C$ until processed for analysis. Tissue samples: selected tissues (injection site, liver, kidney, spleen, LNN) were removed from euthanised animals (isofluorane inhaled anaesthetic followed by exsanguination via abdominal aorta) after 4 h, 48 h or 7 days, individually weighed, and then stored at $\leq -15\ ^{\circ}C$ until processed for analysis.

2.5. Tissue and plasma extraction

ODN were extracted from tissues pieces (∼100 mg) or plasma (100 μl). Typically, 1.25 μg of internal standard

(IS) was added to the samples before the extraction. Tissue or plasma were lysed using a Quantum Appligene (Q Biogen) Bio 101 Savant FP120 Fast-Prep Cell Disruptor and Quantum Appligene (Q Biogen) Bio 101 Matrix Green Homogenisation Beads for 45 s at speed 5. After incubation for 2 h at 55 °C in proteinase K buffer (1 mg/ml proteinase K in 30 mM Tris pH 8; 30 mM EDTA; 5% Tween 20; 0.5% Triton X 100; 800 mM guanidinium HCl; either with 50 mM DTT or without DTT) samples were applied to phenol extraction, the resulting supernatant was applied on a SAX-SPE column (Agilent-Accubond II SAX cartridge; 100 mg, 1 ml; Part No. 188-1610) using SAX buffer (25 mM Tris/HCL, pH 9.00, 25 M KCl, 20% acetonitrile, either with 1 mM DTT or without DTT) eluted with the same buffer containing 1 M NaBr and subsequently applied to a RP-SPE column (Glen Research Poly Pak Barrel, 125 mg; No. 60-2100-30) using RP-dilution buffer (25 mM Tris/HCl, pH 9.0; 0.5 M KCl; 1 M NaBr either with 1 mM DTT or without DTT). The eluate of the RP-column was dialyzed and applied to CGE-UV and MALDI-TOF.

2.6. Capillary gel electrophoresis

For CGE, a PACE MDQ system (Beckman) equipped with the Karat 5.0 software (Beckman) was used. The desalted sample solutions from tissue or plasma extraction were injected electrokinetically into a gel-filled capillary from the sample side using water pre-injection and electropherograms were generated. Concentrations of the different metabolites N-1 to N-6 were determined individually using the instrument software and integration parameters described below. Due to technical reasons for peak integration of the recorded electropherograms, metabolites smaller than N-6 were listed as a total. Concentrations of CPG 7909 and metabolites were calculated using the following formula: ODN concentration [mg ODN/kg tissue] = A/B, where A = extinction coefficient of analyte × corrected area of analyte × amount of standard) [μg] × 1000, and B = extinction coefficient of standard) × corrected area of standard) × tissue weight [mg]. Data was expressed as mean ± standard deviation (S.D.) of values obtained with three individual samples for each given time and dose. The electrophoretic conditions were: (i) capillary: eCAP DNA, neutral, 30 cm, 100 μm I.D. (Beckman # 477477); (ii) capillary temperature: 25 °C; (iii) sample storage temperature: 10 °C; (iv) gel: ssDNA 100 R (Beckman # 477621); (v) buffer: Tris/boric acid/EDTA buffer containing 7 M urea (Beckman # 338481); (vi) detection wavelength: 260 nm; (vii) separation voltage: 300 V/cm; (viii) injection time: 4–10 s; (ix) injection voltage: 10 kV; (x) run time: 45 min; (xi) data acquisition rate: 4 pt./s. The relative migration time and relative area percent of any electrophoretic peak that was >3× signal:noise ratio was recorded. Peak heights of between 3× and 10× signal:noise were recorded as not quantifiable. Electropherograms were analyzed by integration using the Beckman Karat Software (Version 5.0), and the corrected peak area of the main peak for each sample was recorded. All described ODN concentrations were calculated using area under the curve integrations of the CGE electropherograms comparing a defined amount of internal standard ODN (IS) to the analyte CPG 7909. Typical integration parameters were: (i) threshold: 300; (ii) peak width: 1.0; (iii) peak sensitivity: 300.

2.7. MALDI-TOF

The desalted samples containing CPG 7909 and its metabolites were analyzed on a linear Voyager DE MALDI-TOF mass spectrometer (Applied Biosystems) with a delayed extraction source, a nitrogen laser at 337 nm wavelength and a 1.2 m flight tube. The sample matrix was 3-hydroxypicolinic acid containing diammonium citrate. The instrument settings were: (i) voltage: 25 kV; (ii) grid voltage: 95.4%; (iii) guide wire: 0.1%; (iv) delay time: 1100–1200 ns. The spectra of the ODN samples were calibrated externally on the same plate under identical conditions using a set of standard ODN of known molecular weights. Molecular masses were recorded and compared to possible sequences of metabolites of corresponding lengths. All possible sequences for a given mass were listed.

3. Results

3.1. Development of a modified SPE method

We modified a previously published ODN extraction method [48] by adding DTT in different concentrations to the buffers. Human plasma or mouse liver lysates spiked with CPG 7909 and internal standard were extracted using either the unmodified or the modified SPE method. MALDI-TOF analysis of the extracts showed that oxidation of the PS-ODN occurred during the extraction process in both matrices (plasma and liver lysate), resulting in significantly reduced sensitivity of MALDI-TOF (Fig. 1). This oxidative process could be prevented by addition of DTT as a reducing agent to the extraction buffers (Fig. 2). Quantification of CPG 7909 by integration of CGE-UV electropherograms, using a standard curve of the internal standard (IS), indicated linearity of the extractions of CPG 7909 in the relevant concentration range (10–180 mg/kg) (Fig. 3). Furthermore, the extraction efficacy from spiked plasma and liver lysate was shown to be similar for metabolites N-1 to N-6 compared to the parent compound at concentrations 1–25 μg/ml (Figs. 4 and 5).

3.2. Quantification of CPG 7909 and metabolites in plasma

At both 10 min and 2 h after SC injection of mice with 500 μg CPG 7909, the detected concentrations of total ODN

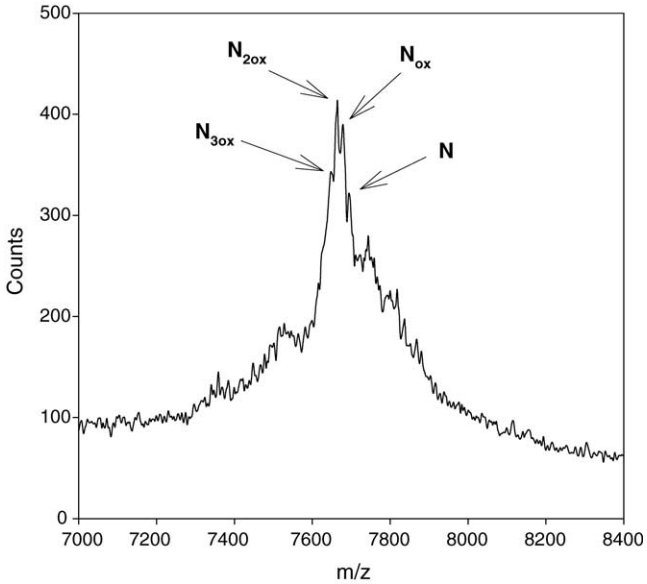

Fig. 1. MALDI-TOF mass spectrum of rat liver lysate spiked with CPG 7909 (N), which was extracted using unmodified methods.

was 20–25 μg/ml, however this dropped to 3 μg/ml by 4 h and was below the detection limit (<0.12 μg/ml) by 8 h (Fig. 6). Significant amounts of metabolic products were detected as early as 10 min, with full-length CPG 7909 representing only ∼65–70% of total detected ODN. The degradation products, which were predominantly N-1 metabolites (24–27% of total detected ODN), remained constant from 10 min to 4 h. Thus, smaller metabolites were a minority, and even after 4 h only a very small fraction of ODN detected in plasma was smaller than N-6 (∼3%) (Fig. 6).

3.3. Tissue distribution, dose dependency in mouse

After SC injection of mice with the highest dose of CPG 7909 (25 mg/kg), the detected concentrations of total ODN

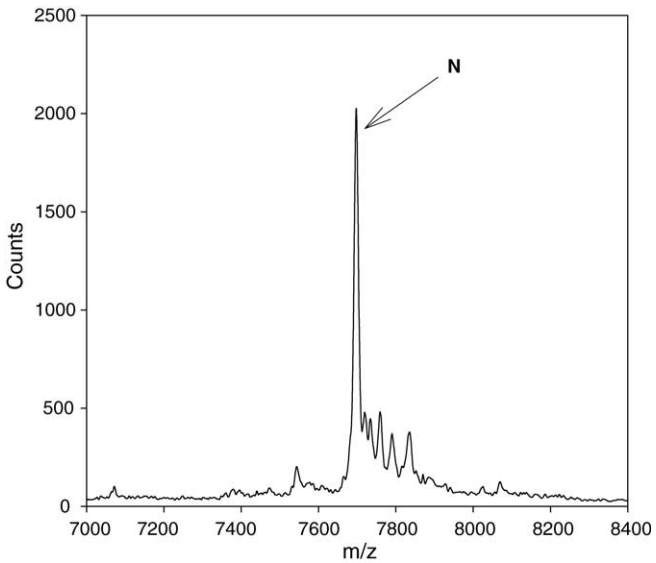

Fig. 2. MALDI-TOF mass spectrum of rat liver lysate spiked with CPG 7909 (N), which was extracted using DTT-modified methods.

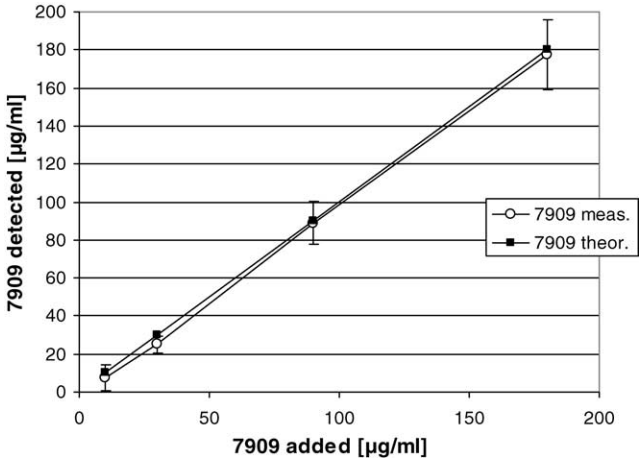

Fig. 3. Standard curve for CPG 7909 recovered from spiked rat liver lysate by SPE. Theoretical values are indicated by closed squares and measured values (means ± S.D.) of three samples are indicated by open circles.

in liver and kidney were similar (∼100 and ∼120 mg/kg respectively) and varied little between 4 h and 7 days. At the three lower doses (2, 5, and 12.5 mg/kg) concentrations in the liver were approximately twice those in the kidney. ODN concentrations remained constant between 4 and 48 h, but had dropped significantly after 7 days (Figs. 7 and 8).

3.4. Tissue distribution in rat

After SC injection of rat with 9 mg/kg CPG 7909, the highest concentrations of CPG 7909 and metabolites were detected in the injection site, ranging from 670 to 432 mg/kg, followed by LLN (122–34 mg/kg), liver (93–44 mg/kg) and kidney (83–48 mg/kg) (Fig. 9). At all time points tested (4, 24 and 72 h), the highest absolute amounts of CPG 7909 and metabolites were found in the liver (31–16%), closely followed by the injection site (23–11%). Kidney and LLN both contained relatively low quantities

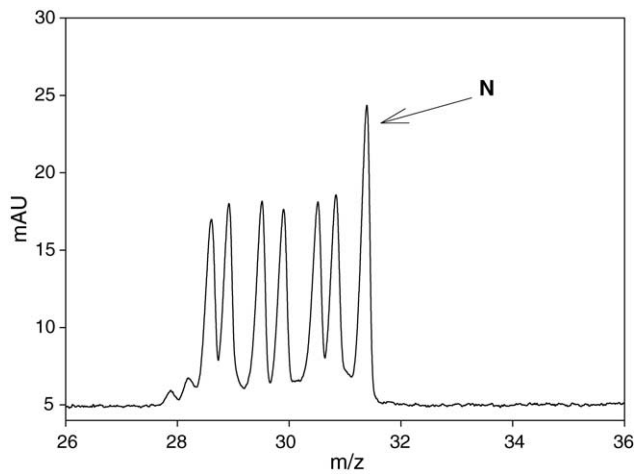

Fig. 4. CGE electropherogram (at 254 nm) of CPG 7909 (N) and six impurity markers (N-1 to N-6) before SPE.

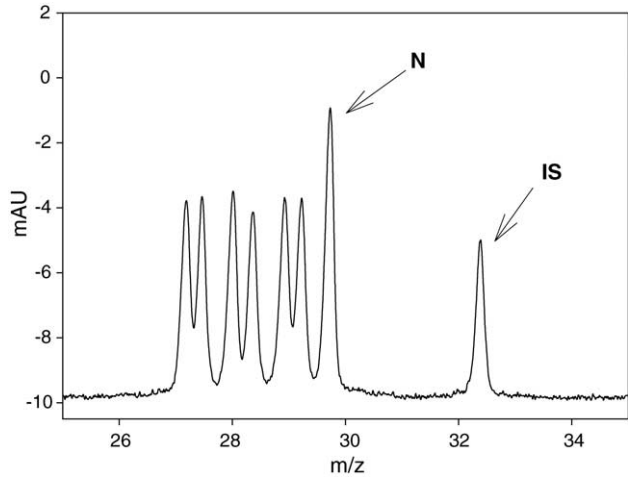

Fig. 5. CGE electropherogram (at 254 nm) of CPG 7909 (N) and six impurity markers (N-1 to N-6) and added internal standard ODN (IS) after SPE.

of the total CPG 7909 and metabolites (7–3 and 1% respectively) (Fig. 10).

3.5. Metabolite distribution

In all organs, the highest proportion of full-length CPG 7909 (N) was detected at the earliest time point (4 h), but this was never more than half of the total material detected: injection site (50%), LLN (40%), liver (33%) and kidney (18%). A large proportion of the ODN detected, especially at the latest time point (72 h), were smaller than N-6: kidney (44%), liver (29%), LLN (16%) and injection site (8%) (Fig. 11 and Table 1). The identified metabolites appeared to be similar in the four different tissues. Base deletions were predominantly detected at the 3′end, however a proportion of the metabolites N-1 to N-6 showed deletions of one or two bases at the 5′end, resulting in at least three different metabolites of the same length (Table 2). Differences in intensity of the respective metabolite peaks in the MALDI-TOF spectra were attributed to

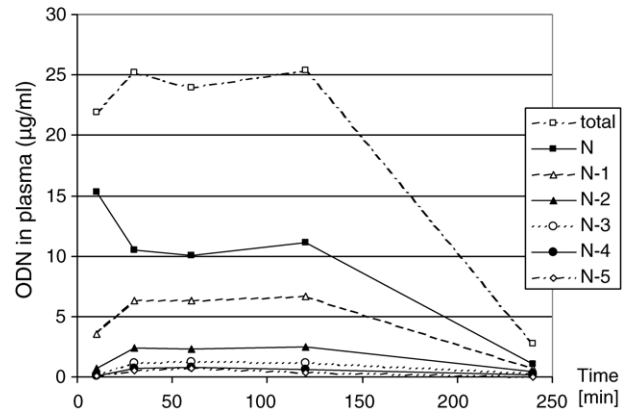

Fig. 6. Quantities of CPG 7909 and major metabolites in mouse plasma at various times after a single SC bolus injection at 25 mg/kg. Each point represents mean values for three mice.

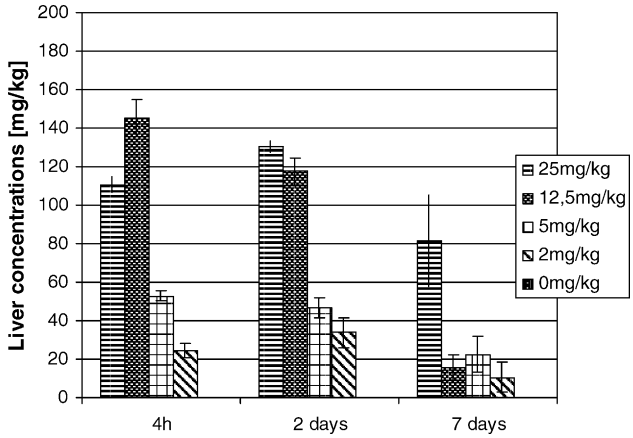

Fig. 7. CPG 7909 and metabolites detected by CGE-UV in mouse liver recovered at different times from Balb/c mice injected with different doses of CPG 7909. Each bar represents mean values ($n = 3$) and vertical lines represent standard deviations.

an accumulation of signals at a specific molecular weight for metabolites of the same length (Fig. 12 and Table 2, see N-5). Some metabolites of the same length but different sequence show exactly the same molecular mass, resulting in a single peak in the MALDI-TOF (Fig. 12, see N-5 in kidney). Other metabolites show different masses (Table 2, see N-3, N-4 and N-6), which results in double or triple peaks of lower intensity (Fig. 12). The shortest metabolites that could be detected in tissues were approximately nine bases long.

4. Discussion

4.1. Improved ODN extraction method

We have successfully developed a method for isolation of CPG 7909 from mouse tissues or human plasma that prevents the previously reported problem [19,43] of oxidation of the phosphorothioate bonds of the PS-ODN, which

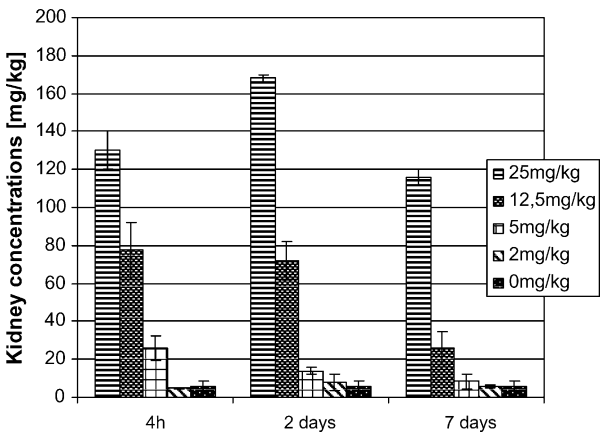

Fig. 8. CPG 7909 and metabolites detected by CGE-UV in mouse kidney recovered at different times from Balb/c mice injected with different doses of CPG 7909. Each bar represents mean values ($n = 3$) and vertical lines represent standard deviations.

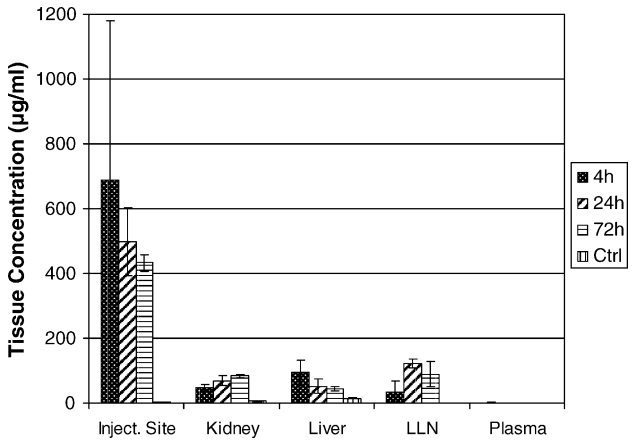

Fig. 9. Concentrations of CPG 7909 and metabolites detected by CGE-UV in rat plasma and tissues at various times after a single SC bolus injection of CPG 7909 at 9.0 mg/kg in a volume of 2.5 ml/kg. Each bar represents mean values for values derived from three animals and vertical lines represent standard deviations. The PBS controls (Ctrl) are means for all three time points.

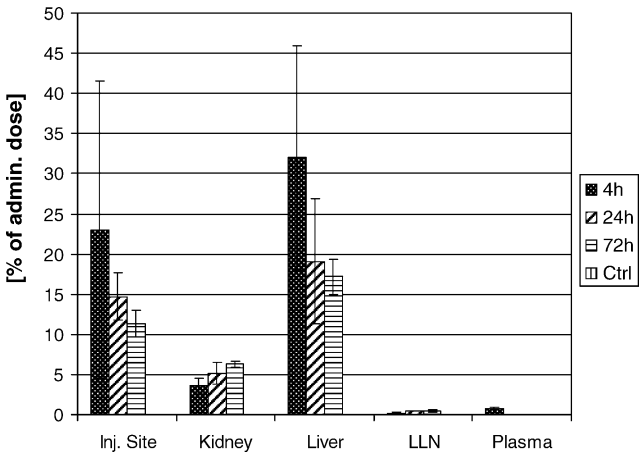

Fig. 10. Percentage of total administered dose represented by CPG 7909 and metabolites in rat plasma and tissues at various times after a single SC bolus injection of CPG 7909 at 9.0 mg/kg in a volume of 2.5 ml/kg. Each bar represents mean values for values derived from three animals and vertical lines represent standard deviations. The PBS controls (Ctrl) are means for all three time points.

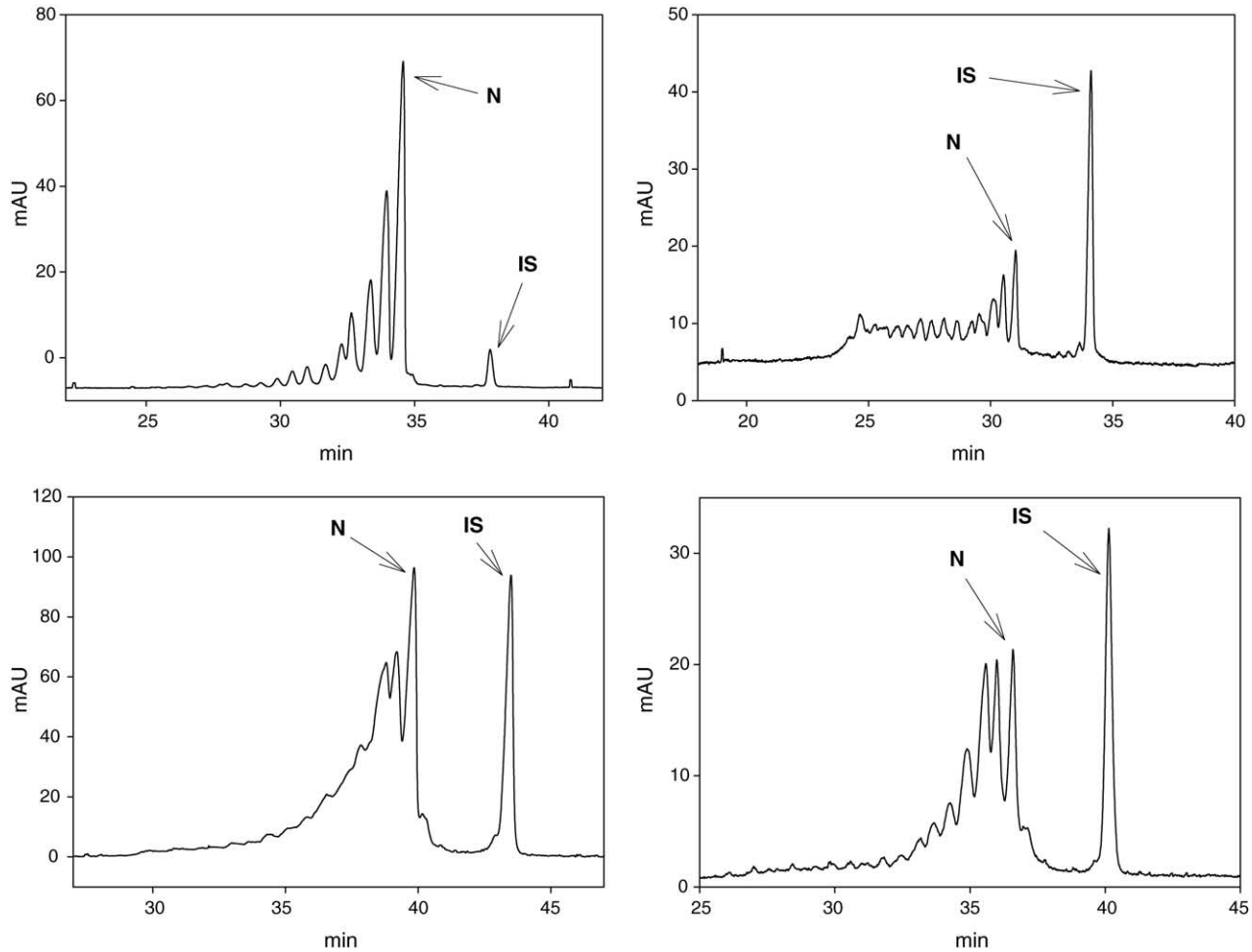

Fig. 11. Electropherograms of CPG 7909 and metabolites in rat tissues after SC administration. Sprague–Dawley rats (n = 3 per time point) were given a single SC bolus injection of 9.0 mg/kg CPG 7909 in a volume of 2.5 ml/kg. At various time points after injection, animals were euthanised and tissues collected. CPG 7909 (N) and metabolites were extracted, CGE-UV electropherograms of injection site (upper left), kidney (upper right), LLN (lower left) and liver (lower right) after 24 h were generated as described in Section 2.

Table 1
Relative quantities of CPG 7909 and metabolites in rat tissues after SC administration

	4 h	24 h	72 h
Injection site			
N	50.4	36.6	30.2
N-1	25.6	23.4	18.2
N-2	6.7	14.0	15.6
N-3	5.5	9.1	11.0
N-4	2.8	5.2	6.9
N-5	1.3	2.8	4.6
N-6	2.1	2.4	3.7
<N-6	6.0	4.9	7.8
Kidney			
N	18.0	9.6	9.2
N-1	16.9	7.5	8.9
N-2	13.5	9.9	10.0
N-3	7.9	5.6	8.2
N-4	7.3	7.8	6.3
N-5	5.8	4.7	5.8
N-6	5.2	6.7	6.5
<N-6	26.0	47.4	44.1
LLN			
N	40.1	23.6	11.6
N-1	23.6	17.3	11.0
N-2	14.3	20.9	17.3
N-3	7.6	10.3	13.1
N-4	4.2	8.7	8.4
N-5	2.3	5.9	8.8
N-6	2.1	4.0	6.9
<N-6	5.7	7.0	16.0
Liver			
N	33.3	11.2	5.6
N-1	23.3	11.8	9.4
N-2	18.3	15.6	14.9
N-3	8.3	11.1	12.3
N-4	3.8	6.6	9.2
N-5	2.7	5.6	9.1
N-6	1.5	3.3	6.7
<N-6	3.6	28.1	28.9

Sprague–Dawley rats ($n = 3$ per time point) were given a single SC bolus injection of 9.0 mg/kg CPG 7909 in a volume of 2.5 ml/kg. At various time points after injection, animals were euthanised and tissues collected. CPG 7909 was extracted and parent compound (N) and metabolites (N-*X*) were quantified by integration of the CGE-UV electropherograms, as described in Section 2. The metabolite distribution is shown as percentage of total detected ODN (%).

significantly complicates metabolite analysis. The conversion consists of an exchange of a sulphur for an oxygen in the phosphate bonds, which leads to a molecular mass change of −16 Da per exchange. This cannot be easily explained by (enzymatic) metabolism processes in the organs and is most likely caused by the SPE procedure [43]. Especially the phenol extraction step appears to contribute to the conversion process, indicating the presence of oxidative agents in these buffers (e.g.: phenol-derivatives with a high oxidative potential, such as benzoquinones). While this conversion does not affect detection and quantification of the ODN by CGE, which does not differentiate between P-S and P-O, it strongly affects mass spectrometric measurements, since the same molecular mass difference is observed between the nucleotides T and C. Hence a TpT dinucleotide with a sulphur–oxygen exchange would display the same molecular mass as a TpC thioate dinucleotide. For an ODN like CPG 7909, which contains several T and C nucleotides, the oxidative processes occurring during established SPE would make it very difficult to analyze the mass spectrometric data. For example, no clear distinction between different 5′ or 3′ metabolites would be possible [19,43,44].

Our modified SPE procedure prevented the oxidation of the phosphorothioate oligonucleotides, greatly enhancing our ability to perform mass spectrometric analysis of the extracted mixture of parent and metabolites. In addition, we were able to show linearity of the extractions of CPG 7909 and metabolites in a concentration range of 10–180 mg/kg, as well as similar extraction efficiencies for all ODN from N to N-6. Stability of the extracted ODN during SPE against degradation and cleavage reactions is demonstrated by the integrity of the IS over the entire process. The improved method should have broad applicability for extraction of any ODN, and may allow better comparison of results between different studies.

4.2. Plasma concentration after SC injection in mice

In mouse plasma, ODN concentrations (CPG 7909 and metabolites as a total) remained almost constant between 10 min and 2 h after SC injection, which agrees with previously published results [19]. This may be explained by a continual supply of ODN from the injection site into the bloodstream. Consequently, plasma concentrations were different, when CPG 7909 was administered IV, peaking directly after injection and decreasing strongly with time (McCluskie et al., unpublished results). The sharp drop in plasma concentration between 2 and 4 h after SC administration may reflect a decreasing supply from the injection site, and is in accordance with the reported plasma half-life (157–186 min) of antisense ODN of similar physico-chemical properties [33].

During the first 4 h of our studies, total ODN comprised about 40% N, 24–27% N-1 metabolites and only small amounts of smaller metabolites (ca. 3% were smaller than N-6). Apparently, the first degradation step occurs very quickly, either at the injection site or in the plasma itself, but further degradation seems to be slower. Explanations include the inhibition of nucleases [15] and/or the distribution of Rp and Sp phosphorothioate diastereoisomeres, with their significantly different nuclease resistance [39–41]. The limited appearance of smaller metabolites argues for predominant cleavage by exonucleases. Since the major metabolites of CPG 7909 detected in plasma (N-1, N-2 and N-3) display strong immunomodulatory properties (Vollmer et al., unpublished results), and together with N constitute >95% of total detected ODN, the ODN in the plasma circulating for the first 2 h can be considered fully immunomodulatory.

Table 2
ODN masses detected in the MALDI-TOF correlated to possible metabolite sequences

7909	TCG TCG TTT TGT CGT TTT GTC GTT	7698.0 Da
N-1	TCG TCG TTT TGT CGT TTT GTC GT	7377.8 Da
	CG TCG TTT TGT CGT TTT GTC GTT	7377.8 Da
N-2	G TCG TTT TGT CGT TTT GTC GTT	7072.5 Da
	CG TCG TTT TGT CGT TTT GTC GT	7057.5 Da
	TCG TCG TTT TGT CGT TTT GTC G	7057.5 Da
N-3	TCG TCG TTT TGT CGT TTT GTC	6712.3 Da
	CG TCG TTT TGT CGT TTT GTC G	6737.3 Da
	G TCG TTT TGT CGT TTT GTC GT	6752.3 Da
N-4	TCG TCG TTT TGT CGT TTT GT	6407.1 Da
	CG TCG TTT TGT CGT TTT GTC	6392.0 Da
	G TCG TTT TGT CGT TTT GTC G	6432.0 Da
N-5	TCG TCG TTT TGT CGT TTT G	6086.8 Da
	CG TCG TTT TGT CGT TTT GT	6086.8 Da
	G TCG TTT TGT CGT TTT GTC	6086.8 Da
N-6	TCG TCG TTT TGT CGT TTT	5741.5 Da
	CG TCG TTT TGT CGT TTT G	5766.5 Da
	G TCG TTT TGT CGT TTT GT	5781.5 Da
N-7	TCG TCG TTT TGT CGT TT	5421.3 Da
	CG TCG TTT TGT CGT TTT	5421.3 Da
	G TCG TTT TGT CGT TTT G	5461.2 Da

Metabolites are grouped according to length and detected masses with more than one possible corresponding metabolite sequence are underlined. All listed ODN are phosphorothioates. For clarity reasons, base sequences are grouped into base triplets.

4.3. Tissue distribution after SC injection in mice

When using increasing doses in mouse studies, no proportional increase in liver concentrations was observed for the 12.5 and 25 mg/kg doses, suggesting that tissue saturation was reached at doses above 12.5 mg/kg. However, by 7 days after administration of the 12.5 mg/kg dose, concentrations in the liver had dropped, indicating the end of saturation. In contrast, the kidneys showed significantly lower ODN concentrations after a 12.5 mg/kg dose than after a 25 mg/kg dose, indicating a lack of saturation in the kidney, possibly due to ongoing clearance. However, unpublished data from our laboratory showed no further increase in kidney concentrations after a second 25 mg/kg dose of ODN at day 5, compared to a single 25 mg/kg dose, indicating that saturation of the kidney can also be reached, at least at ODN doses of 25 mg/kg or higher. Spleen samples from control rats and mice (injected with PBS) consistently showed high background levels, which was possibly caused by co-purifying spleen-specific nucleotides or peptides since no background was detected in another lymphoid tissue (lymph nodes). ODN concentrations in the spleen were lower than those in the liver and kidney and appeared to be independent of dose (~40 mg/kg at all dose levels after 48 h), indicating saturation of this tissue at the dose levels tested. However, enlargement of the spleen was observed, which accounts for an increase in total ODN amount in the organ at high doses and later time points (up to five-fold increase in tissue weights after 7 days at the high doses, unpublished results). Unlike the rat, no increase in kidney concentration was observed over time in mice. This may be due to the higher metabolic rate in mice, which can be two to three times higher than that in rat tissue [22,45].

4.4. Tissue distribution after SC injection in rat

The high local concentrations and total amounts of ODN detected in the injection site at all time points indicate a long retention time in this site. While ODN concentrations were lower in the liver than the injection site, the liver contained the highest absolute amount due to its large size. Together, the injection site and liver may function as ODN depots and may account for sustained concentrations of ODN in the plasma and other organs.

The kinetics of ODN clearance from the injection site, liver, kidney and LLN appeared to be significantly different. Whereas ODN concentrations in the injection site and liver dropped over time, those in the kidney increased slightly, suggesting clearance of ODN from the injection site and liver with subsequent distribution to the kidney. While distribution to the liver and kidney was most likely via the circulatory system, this does not appear to be the case for ODN found in the lymph nodes. A significant

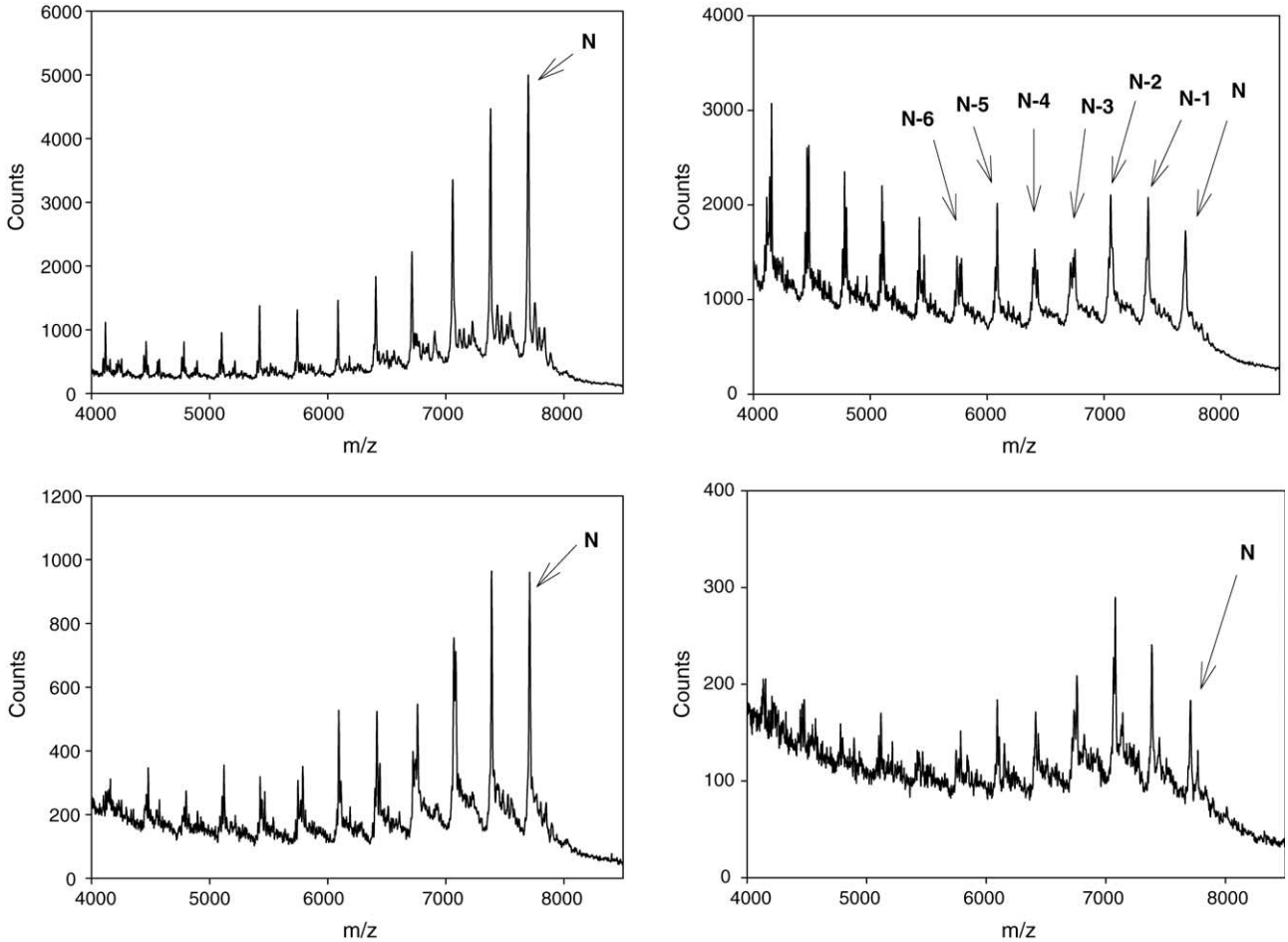

Fig. 12. MALDI-TOF spectra of CPG 7909 and metabolites in rat tissues after SC administration. Sprague–Dawley rats ($n = 3$ per time point) were given a single SC bolus injection of 9.0 mg/kg CPG 7909 in a volume of 2.5 ml/kg. At various time points after injection, animals were euthanised and tissues collected. CPG 7909 (N) and metabolites (N-*X*) were extracted, MALDI-TOF spectra of injection site (upper left), kidney (upper right), LLN (lower left) and liver (lower right) after 24 h were generated as described in Section 2.

increase in ODN concentration was observed between 4 h and 24 h in LLN. Using radiolabeled drug, high levels are also found in the draining, but not the non-draining lymph nodes (McCluskie et al., unpublished results), suggesting transport from the injection site via the lymphatic system.

With the significant exception of the kidney concentrations, these results are in agreement with biodistribution data obtained at the same dose level using a [^{3}H] radiolabeled probe (McCluskie et al., unpublished results). In kidney, the CPG 7909 concentrations measured by CGE-UV detection were only one-third of the concentration measured by radiolabel detection. These differences may be due to the two different detection methods used in the studies. Detection by CGE-UV only picks up oligonucleotides larger than six bases, whereas radiolabel detection picks up even very small ODN metabolites, which would be expected to pass through the kidney, as well as small molecules such as water, urea or H_2CO_3 that may have incorporated radiolabel through anabolism. This finding highlights the necessity of considering the detection method when analysing and comparing PK data.

ODN distribution patterns appear to be similar after SC or IV administration, with the obvious exception that no injection site depot is formed in case of IV injection, resulting in slightly higher ODN concentrations in the organs and lower concentrations in the lymph nodes compared to SC injection (McCluskie et al., unpublished results).

For injection site samples recovered after 4 h, the calculated concentrations of ODN varied from 159 to 1124 mg/kg between animals. This high variability likely reflects the fact that drug can distribute through a large and variable SC space and only fractions of the injection site tissue samples were analyzed. However, the mean values were in agreement with values obtained by other techniques.

4.5. Metabolism of CPG 7909

The degree of degradation varied with time and between tissues, but with similar patterns for the two species. Generally, the proportion of smaller metabolites increased over time, with base deletions occurring preferentially at the

3′end, indicating degradation of CPG 7909 predominantly by 3′exonucleases. However, a proportion of the identified metabolites showed deletions of one or two bases at the 5′end, indicating endonuclease or 5′exonuclease activity, resulting in at least three different metabolites of the same length and sometimes the same molecular weight but different sequence. All possible sequences of the detected metabolite masses N-1 to N-6 were listed for the analyzed tissues and the identified metabolites appeared to be similar in all sites. Liver and kidney showed a much higher percentage of metabolites than injection site and local lymph nodes, where 3′-exonuclease activity as well as endonuclease activity appeared to be lower. This may be due to different organ distribution of degrading enzymes [29] rather than a reflection of differences in the disposition properties of the individual metabolites. We have no indication for differential distribution pathways for different metabolites.

Since small metabolites are less likely to contain the intact hexamer human Toll-like receptor 9 recognition motif (GTCGTT) [2], only a fraction of short metabolites are expected to show immunomodulatory activity. Although our SPE method can extract and quantify spiked ODN as short as six bases (unpublished data), the shortest CPG 7909 metabolites detected in organs recovered from animals were approximately nine bases, which is in line with previous findings [29].

The conclusions of this study may have significance for CPG 7909 clinical studies. CPG 7909 is typically administered SC to cancer patients once weekly at doses less than 1 mg/kg. In the present study, no ODN (parent or metabolite) is detected by CGE-UV in mouse kidney (the organ that achieved highest concentrations) by 7 days, even at the 5 mg/kg dose, suggesting that drug accumulation is not likely to occur with repeated weekly doses of CPG 7909 at the doses used in human trials. Furthermore, the pattern and kinetics of ODN degradation indicate that most of the metabolites present in the kidney would not be immunostimulatory. Unfortunately, CGE-UV was unable to quantify metabolites in tissues after single subcutaneous doses below 2 mg/kg. This means that it will not be possible to analyze metabolites in human PK samples by current CGE-UV methods. However, the tissue distribution data obtained by more sensitive, radioactive methods at doses in the range of human clinical trials strongly support our CGE-UV data (McCluskie et al., unpublished results). We therefore expect the general metabolism pathways as described herein (doses 2–25 mg/kg) to be indicative for the low doses used in clinical trials (<1 mg/kg).

Acknowledgement

This work was supported by DARPA (DAAD19-03-C-0002).

References

[1] Hartmann G, Weeratna RD, Ballas ZK, Payette P, Blackwell S, Suparto I, et al. Delineation of a CpG phosphorothioate oligodeoxynucleotide for activating primate immune responses in vitro and in vivo. J Immunol 2000;164:1617–24.
[2] Hartmann G, Krieg AM. Mechanism and function of a newly identified CpG DNA motif in human primary B cells. J Immunol 2000;164:944–53.
[3] Krieg AM. Antitumor applications of stimulating toll-like receptor 9 with CpG oligodeoxynucleotides. Curr Oncol Rep 2004;6:88–95.
[4] Cooper CL, Davis HL, Morris ML, Efler SM, Krieg AM, Li Y, et al. Safety and immunogenicity of CPG 7909 injection as an adjuvant to Fluarix influenza vaccine. Vaccine 2004;22:3136–43.
[5] Cooper CL, Davis HL, Morris ML, Efler SM, Al Adhami M, Krieg AM, et al. CPG 7909, an immunostimulatory TLR9 agonist oligodeoxynucleotide, as adjuvant to Engerix-B HBV vaccine in healthy adults: a double-blind Phase I/II study. J Clin Immunol 2004;24(6):693–701.
[6] Siegrist CA, Pihlgren M, Tougne C, Efler SM, Morris ML, Al Adhami MJ, et al. Co-administration of CpG oligonucleotides enhances the late affinity maturation process of human anti-hepatitis B vaccine response. Vaccine 2004;23(5):615–22.
[7] Agrawal S, Temsamani J, Tang JY. Pharmacokinetics, biodistribution, and stability of oligodeoxynucleotide phosphorothioates in mice. Proc Natl Acad Sci USA 1991;88:7595–9.
[8] Goodarzi G, Watabe M, Watabe K. Organ distribution and stability of phosphorothioated oligodeoxyribonucleotides in mice. Biopharm Drug Dispos 1992;13:221–7.
[9] Iversen PL, Copple BL, Tewary HK. Pharmacology and toxicology of phosphorothioate oligonucleotides in the mouse, rat, monkey and man. Toxicol Lett 1995;82–83:425–30.
[10] Cossum PA, Sasmor H, Dellinger D, Truong L, Cummins L, Owens SR, et al. Disposition of the 14C-labeled phosphorothioate oligonucleotide ISIS 2105 after intravenous administration to rats. J Pharmacol Exp Ther 1993;267:1181–90.
[11] Sands H, Gorey-Feret LJ, Cocuzza AJ, Hobbs FW, Chidester D, Trainor GL. Biodistribution and metabolism of internally 3H-labeled oligonucleotides I. Comparison of a phosphodiester and a phosphorothioate. Mol Pharmacol 1994;45:932–43.
[12] Agrawal S, Temsamani J, Galbraith W, Tang J. Pharmacokinetics of antisense oligonucleotides 3. Clin Pharmacokinet 1995;28:7–16.
[13] Zhang R, Lu Z, Zhao H, Zhang X, Diasio RB, Habus I, et al. In vivo stability, disposition and metabolism of a "hybrid" oligonucleotide phosphorothioate in rats 1. Biochem Pharmacol 1995;50:545–56.
[14] Crooke RM, Graham MJ, Cooke ME, Crooke ST. In vitro pharmacokinetics of phosphorothioate antisense oligonucleotides. J Pharmacol Exp Ther 1995;275:462–73.
[15] Crooke ST, Graham MJ, Zuckerman JE, Brooks D, Conklin BS, Cummins LL, et al. Pharmacokinetic properties of several novel oligonucleotide analogs in mice. J Pharmacol Exp Ther 1996;277:923–37.
[16] Rifai A, Brysch W, Fadden K, Clark J, Schlingensiepen KH. Clearance kinetics, biodistribution, and organ saturability of phosphorothioate oligodeoxynucleotides in mice. Am J Pathol 1996;149:717–25.
[17] Cossum PA, Truong L, Owens SR, Markham PM, Shea JP, Crooke ST. Pharmacokinetics of a 14C-labeled phosphorothioate oligonucleotide, ISIS 2105, after intradermal administration to rats. J Pharmacol Exp Ther 1994;269:89–94.
[18] Saijo Y, Perlaky L, Wang H, Busch H. Pharmacokinetics, tissue distribution, and stability of antisense oligodeoxynucleotide phosphorothioate ISIS 3466 in mice. Oncol Res 1994;6:243–9.
[19] Phillips JA, Craig SJ, Bayley D, Christian RA, Geary R, Nicklin PL. Pharmacokinetics, metabolism, and elimination of a 20-mer phosphorothioate oligodeoxynucleotide (CGP 69846A) after intravenous

and subcutaneous administration. Biochem Pharmacol 1997;54: 657–68.

[20] Nicklin PL, Bayley D, Giddings J, Craig SJ, Cummins LL, Hastewell JG, et al. Pulmonary bioavailability of a phosphorothioate oligonucleotide (CGP 64128A): comparison with other delivery routes. Pharm Res 1998;15:583–91.

[21] Templin MV, Levin AA, Graham MJ, Aberg PM, Axelsson BI, Butler M, et al. Pharmacokinetic and toxicity profile of a phosphorothioate oligonucleotide following inhalation delivery to lung in mice. Antisense Nucl Acid Drug Dev 2000;10:359–68.

[22] Geary RS, Leeds JM, Fitchett J, Burckin T, Truong L, Spainhour C, et al. Pharmacokinetics and metabolism in mice of a phosphorothioate oligonucleotide antisense inhibitor of C-raf-1 kinase expression. Drug Metab Dispos 1997;25:1272–81.

[23] Geary RS, Leeds JM, Henry SP, Monteith DK, Levin AA. Antisense oligonucleotide inhibitors for the treatment of cancer. 1. Pharmacokinetic properties of phosphorothioate oligodeoxynucleotides. Anticancer Drug Des 1997;12:383–93.

[24] Nolting A, DeLong RK, Fisher MH, Wickstrom E, Pollack GM, Juliano RL, et al. Hepatic distribution and clearance of antisense oligonucleotides in the isolated perfused rat liver. Pharm Res 1997; 14:516–21.

[25] Peng B, Andrews J, Nestorov I, Brennan B, Nicklin P, Rowland M. Tissue distribution and physiologically based pharmacokinetics of antisense phosphorothioate oligonucleotide ISIS 1082 in rat. Antisense Nucl Acid Drug Dev 2001;11:15–27.

[26] Grindel JM, Musick TJ, Jiang Z, Roskey A, Agrawal S. Pharmacokinetics and metabolism of an oligodeoxynucleotide phosphorothioate (GEM91) in cynomolgus monkeys following intravenous infusion 1. Antisense Nucl Acid Drug Dev 1998;8:43–52.

[27] Yu RZ, Geary RS, Leeds JM, Watanabe T, Fitchett JR, Matson JE, et al. Pharmacokinetics and tissue disposition in monkeys of an antisense oligonucleotide inhibitor of Ha-ras encapsulated in stealth liposomes. Pharm Res 1999;16:1309–15.

[28] Yu RZ, Geary RS, Leeds JM, Watanabe T, Moore M, Fitchett J, et al. Comparison of pharmacokinetics and tissue disposition of an antisense phosphorothioate oligonucleotide targeting human Ha-ras mRNA in mouse and monkey. J Pharm Sci 2001;90:182–93.

[29] Geary RS, Matson J, Levin AA. A nonradioisotope biomedical assay for intact oligonucleotide and its chain-shortened metabolites used for determination of exposure and elimination half-life of antisense drugs in tissue. Anal Biochem 1999;274:241–8.

[30] Bayever E, Iversen PL, Bishop MR, Sharp JG, Tewary HK, Arneson MA, et al. Systemic administration of a phosphorothioate oligonucleotide with a sequence complementary to p53 for acute myelogenous leukemia and myelodysplastic syndrome: initial results of a phase I trial.. Antisense Res Dev 1993;3:383–90.

[31] Bishop GA, Hsing Y, Hostager BS, Jalukar SV, Ramirez LM, Tomai MA. Molecular mechanisms of B lymphocyte activation by the immune response modifier R-848. J Immunol 2000;165:5552–7.

[32] Glover JM, Leeds JM, Mant TG, Amin D, Kisner DL, Zuckerman JE, et al. Phase I safety and pharmacokinetic profile of an intercellular adhesion molecule-1 antisense oligodeoxynucleotide (ISIS 2302). J Pharmacol Exp Ther 1997;282:1173–80.

[33] Yu RZ, Geary RS, Watanabe TA, Levin AA, Schoenfeld SL. Pharmacokinetic properties in humans. Carlsbad, CA: Isis Pharmaceuticals, Inc. In: Crooke ST, editor. Antisense drug technology. New York, NY: Marcel Dekker, Inc.; 2001. p. 183–200.

[34] Zhang R, Yan J, Shahinian H, Amin G, Lu Z, Liu T, et al. Pharmacokinetics of an anti-human immunodeficiency virus antisense oligodeoxynucleotide phosphorothioate (GEM 91) in HIV-infected subjects. Clin Pharmacol Ther 1995;58:44–53.

[35] Srinivasan SK, Tewary HK, Iversen PL. Characterization of binding sites, extent of binding, and drug interactions of oligonucleotides with albumin. Antisense Res Dev 1995;5:131–9.

[36] Temsamani J, Tang JY, Padmapriya A, Kubert M, Agrawal S. Pharmacokinetics, biodistribution, and stability of capped oligodeoxynucleotide phosphorothioates in mice. Antisense Res Dev 1993;3: 277–84.

[37] Temsamani J, Roskey A, Chaix C, Agrawal S. In vivo metabolic profile of a phosphorothioate oligodeoxyribonucleotide. Antisense Nucl Acid Drug Dev 1997;7:159–65.

[38] Gilar M, Belenky A, Budman Y, Smisek DL, Cohen AS. Study of phosphorothioate-modified oligonucleotide resistance to 3′-exonuclease using capillary electrophoresis. J Chromatogr B Biomed Sci Appl 1998;714:13–20.

[39] Spitzer S, Eckstein F. Inhibition of deoxyribonucleases by phosphorothioate groups in oligodeoxyribonucleotides. Nucl Acids Res 1988; 16:11691–704.

[40] Krieg AM, Guga P, Stec W. P-chirality-dependent immune activation by phosphorothioate CpG oligodeoxynucleotides. Oligonucleotides 2003;13:491–9.

[41] Gilar M, Belenky A, Budman Y, Smisek DL, Cohen AS. Impact of 3′-exonuclease stereoselectivity on the kinetics of phosphorothioate oligonucleotide metabolism. Antisense Nucl Acid Drug Dev 1998;8:35–42.

[42] Iversen PL, Mata J, Tracewell WG, Zon G. Pharmacokinetics of an antisense phosphorothioate oligodeoxynucleotide against rev from human immunodeficiency virus type 1 in the adult male rat following single injections and continuous infusion. Antisense Res Dev 1994; 4:43–52.

[43] Cohen AS, Bourque AJ, Wang BH, Smisek DL, Belenky A. A nonradioisotope approach to study the in vivo metabolism of phosphorothioate oligonucleotides. Antisense Nucl Acid Drug Dev 1997; 7:13–22.

[44] Gaus HJ, Owens SR, Winniman M, Cooper S, Cummins LL. On-line HPLC electrospray mass spectrometry of phosphorothioate oligonucleotide metabolites. Anal Chem 1997;69:313–9.

[45] Graham MJ, Crooke ST, Lemonidis KM, Gaus HJ, Templin MV, Crooke RM. Hepatic distribution of a phosphorothioate oligodeoxynucleotide within rodents following intravenous administration. Biochem Pharmacol 2001;62:297–306.

[46] Griffey RH, Greig MJ, Gaus HJ, Liu K, Monteith D, Winniman M, et al. Characterization of oligonucleotide metabolism in vivo via liquid chromatography/electrospray tandem mass spectrometry with a quadrupole ion trap mass spectrometer. J Mass Spectrom 1997;32:305–13.

[47] Yu RZ, Geary RS, Monteith DK, Matson J, Truong L, Fitchett J, et al. Tissue disposition of 2′-O-(2-methoxy) ethyl modified antisense oligonucleotides in monkeys. J Pharm Sci 2004;93:48–59.

[48] Leeds JM, Graham MJ, Truong L, Cummins LL. Quantitation of phosphorothioate oligonucleotides in human plasma. Anal Biochem 1996;235:36–43.